Fast classification of drones and birds with an LSTM network applied to 1D phase data

Mark A. Bell
SUPA School of Physics & Astronomy
University of St Andrews
St Andrews, Scotland
mab31@st-andrews.ac.uk

Samiur Rahman
SUPA School of Physics & Astronomy
University of St Andrews
St Andrews, Scotland
sr206@st-andrews.ac.uk

Duncan A. Robertson
SUPA School of Physics & Astronomy
University of St Andrews
St Andrews, Scotland
dar@st-andrews.ac.uk

***Abstract*—This study investigates a new type of drone classifier based on Long Short-Term Memory (LSTM) networks. As a real-time surveillance system, the classification time of a drone detection radar is crucial. The motivation for this work is to develop a classification framework which has low latency in terms of data processing for the algorithm input. Theoretical modeling of a rotary wing drone and a bird wing flapping returns were done first to exhibit the difference in the patterns of the respective phase progressions. Then, 94 GHz experimental trial data containing 4800 sequences of drones, birds, noise and clutter were used to create a diverse training dataset of 1D phase data for supervised learning. A stacked LSTM network with tuned hyperparameters was generated to reduce the possible overfitting from a simple LSTM model. Validation accuracy of 98.1% was achieved for 2-class classification of drone and non-drone. Further performance assessment was then done with 30 unseen test data, where the network was able to correctly classify all the sequences. It is ascertained that this method can be ~10 times faster than a spectrogram based classification model, which requires additional Fast Fourier Transform (FFT) operations.**

Keywords—Radar, FMCW, drone, bird, neural network, LSTM, millimeter wave

I. Introduction

Radar is widely used in the surveillance and tracking of airborne targets, with the advantage of being able to operate in all weather and light conditions. The recent advancement in the affordable commercial drone market has also established the need for reliable monitoring sensors for these objects. Therefore, detection and classification of drones using radars has been at the forefront of research and development in the past few years [1]–[4].

Notable progress in computational power has opened the path for advanced machine learning and deep learning based classification techniques, which have been widely explored for drone and bird classification algorithm development. Machine learning classifiers based on feature extraction from the radar micro-Doppler data can provide high accuracy [5]–[8]. Machine learning techniques can suffer from computationally expensive extraction processes (e.g. a conventional Singular Value Decomposition can be time consuming). Any large computational requirement imposes a potential latency when classifying a drone in real-time. Meanwhile, neural network based models can be more efficient by learning pertinent features during training, hence not requiring them to process the radar data to obtain feature values in real-time. Convolutional Neural Network (CNN) based classification techniques have demonstrated promising results (greater than 90% accuracy) using spectrogram images containing micro-Doppler information [9]–[11]. In [12], a Fully Convolutional Network (FCN), which is a modification of CNN, and also an LSTM based classification technique have been proposed. For LSTM training, a spectrogram was considered as a series of 1D spectra. The classification accuracies were above 97% for 30 dB Signal-to-Noise Ratio (SNR) and above 80% for 10 dB SNR. The models were trained with cluttered and noisy signals.

As spectrogram generation requires multiple FFTs along the time series data, reducing the number of FFT operations for neural network input can notably improve the classification speed. This work describes an LSTM model which utilizes phase information of contiguous range profiles from a coherent Frequency Modulated Continuous Wave (FMCW) radar, eliminating the need for any spectrogram/range-Doppler plot generation. The method can be applied to pulse-Doppler radar data as well. The phase data from the complex raw time series has not been used, as no information on range would be available then. It should be noted that even though 2-channel I-Q data have been used here, a single channel FMCW radar data would also suffice, as the range processed data would be complex after the FFT.

Section II of this paper illustrates the simulated phase returns from a drone and a bird target. Section III describes the LSTM network. Section IV provides information on the training dataset. Section V discusses the classification results and then conclusive remarks are given in the last section.

II. Simulated drone and bird Doppler phase

The phase progressions corresponding to the micro-Doppler returns from a rotary wing drone and a bird have been simulated, based on [13], [14]. The simulation is performed for W-band (94 GHz), as the experimental dataset is from a 94 GHz radar.

For a drone, the geometry of a Phantom 3 Standard quadcopter is considered, as it is quite generic. Rotation rates for each rotor can be defined independently. In this case the values have been selected within the range of 50-200 Hz, which are typical for these types of drones. The Doppler sampling rate is specified to be 15 kHz, to represent an expected Chirp Repetition Frequency (CRF) of an FMCW radar, without imposing too much hardware constraint. The CRF here is not high enough to unambiguously sample the micro-Doppler returns from the fast rotating propeller blades at higher frequencies such as W-band. On the other hand, it has been shown that better Doppler sensitivity can be achieved at this frequency range [15], and also Doppler resolution is finer at higher frequencies for a given integration time. Nonetheless, a phase plot with unambiguous Doppler sampling rate is presented here as well to show its difference from a bird phase plot. A hovering drone is considered to reveal the Doppler returns only from the blades. The experimental dataset contains in-flight data as well. For bird

Science and Technology Facilities Council under grant ST/N006569/1

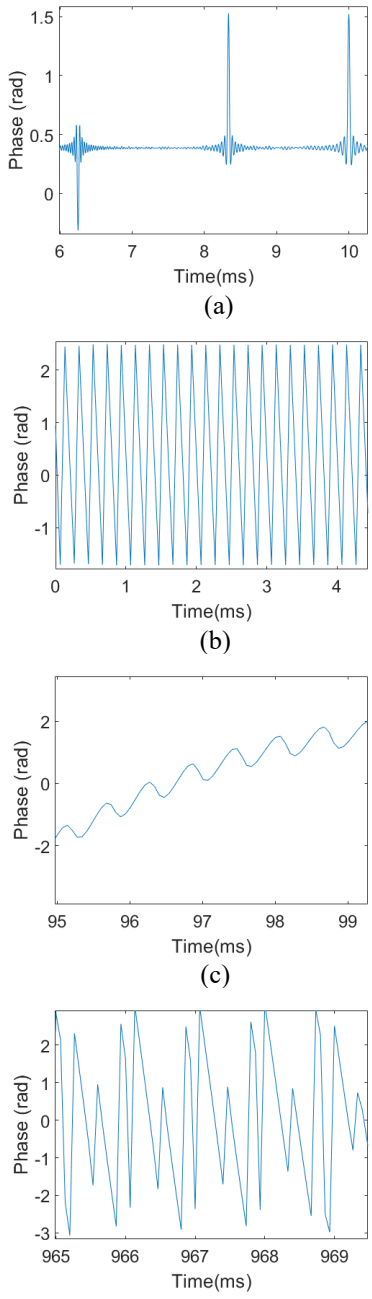

Fig. 1. Simulated 94 GHz phase plots of a (a) quadcopter drone at 200 kHz CRF, (b) quadcopter drone at 15 kHz CRF, (c) bird at 15 kHz CRF, (d) noise at 15 kHz CRF

geometry, the upper arm and forearm lengths are defined as half a meter each, to represent a medium to big sized bird. The flapping frequency is 10 Hz. A real-time 360° surveillance radar will have a very brief exposure to a drone in a single scan. The duration of a phase vector here is 4.27 milliseconds, the length of 64 chirps in time. This roughly corresponds to a single Coherent Processing Interval (CPI) for the 0.5-1 Hz rotation rate of the radar. The CRF of the experimental data is slightly lower, but it is very close to yield similar results.

Fig. 1 shows the simulated phase vector of a drone, bird and noise. The Differences in pattern are observed, which can be attributed to the variations in the micro-Doppler signatures, or lack thereof. The sharp peak on the unambiguously sampled drone phase plot in Fig. 1(a) is due to the propeller blade flash. Fig. 1(b) shows the periodic phase jump due to Doppler when

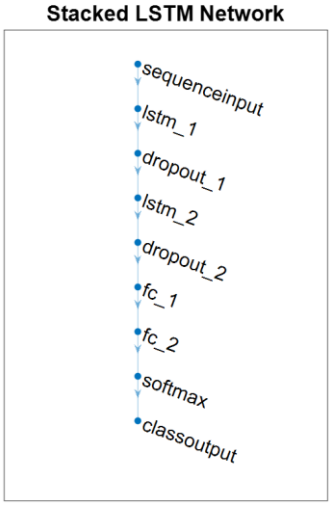

Fig.2. Layer-graph of the stacked LSTM network

TABLE I. STACKED LSTM NETWORK FOR 2-CLASS CLASSIFICATION

Layer	Name	Type	Description
1	'sequenceinput'	Sequence Input	Sequence input with 1 dimension
2	'lstm_1'	LSTM	LSTM with 64 hidden units
3	'dropout_1'	Dropout	25% dropout
4	'lstm_2'	LSTM	LSTM with 32 hidden units
5	'dropout_2'	Dropout	25% dropout
6	'fc_1'	Fully Connected	32 fully connected layer
7	'fc_2'	Fully Connected	2 fully connected layer
8	'softmax'	Softmax	Performs softmax normalisation
9	'classoutput'	Classification Output	Computes cross entropy loss with classes 'Drone' and 'Non-Drone'

under sampled. This is not observed for the bird phase plot in Fig. 1(c), as the wing flapping frequency is comparatively lower, so no aliasing occurs. The simulated results show the potential use of these phase vectors as classifier training data. Some feature extraction based classification might also be done using the phase vectors, but that would involve more computation.

III. STACKED LSTM MODEL

The neural network that was designed used 'stacked' LSTM layers [16], as a simple LSTM network might be prone to overfitting. The network is designed for 2-class classification of drone and non-drone. The layers for this network are shown in Fig. 2 and Table I. A second LSTM network was added following the first. The first LSTM layer outputs in sequence mode, which means it passes on the hidden state at all time steps, whereas the second LSTM network output is the last timestep of the sequence. The goal of this addition was to try and learn more complex features

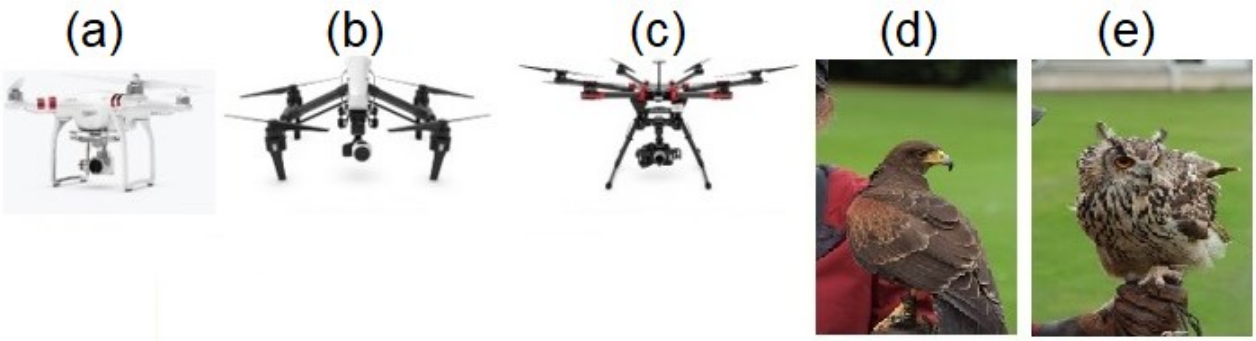

Fig. 3. Images of different targets present in the radar data. A) DJI Phantom 3, b) DJI Inspire 1, c) DJI S900, d) Harris Hawk, e) Indian Eagle Owl

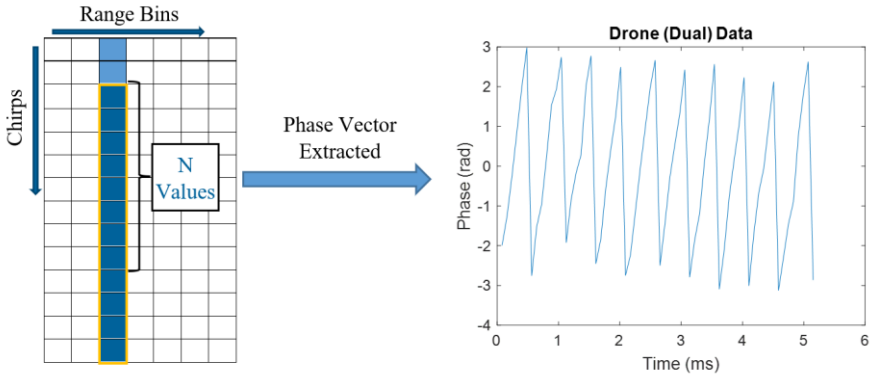

Fig. 4. Diagram showing the process of extracting phase vectors from the complex range transformed data

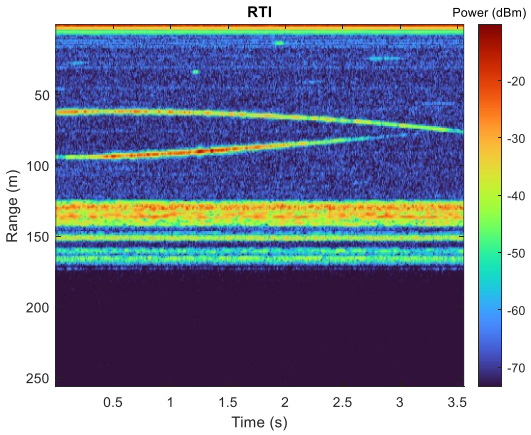

Fig. 5. 94 GHz Range-Time Intensity (RTI) plot example, featuring two drones (DJI Phantom and Inspire) and static clutter. The path of the drones can be identified based on how the range profiles vary over time

from the data, after the first LSTM layer has learnt more basic ones. This would potentially increase the capability of the network to identify more complex sequences. Another fully connected layer was added after this LSTM which features more neurons than just the two used in the 'last-learnable' fully connected layer. Again, this layer is expected to extract more features before the second fully connected. After each of the two LSTM layers, a dropout layer was added. These layers set random inputs to zero during training, based on a set probability factor. The purpose of these dropout layers is to reduce overfitting or dependence on one or two particular neurons. The network was trained using Stochastic Gradient Descent (SGD). MATLAB's implementation of the Stochastic Gradient Descent with Momentum (SGDM) adds a 'momentum' term which changes the amount of information

TABLE II. LSTM TRAINING AND TEST DATA DETAILS

Training Datafile	Target(s)	Velocity range (m/s)
Trial (S900)	DJI S900	-1.8 to 1.6
DJI Inspire 1	DJI Inspire	-5.6 to – 3.9
DJI (Dual)	DJI Inspire, DJI Phantom	-1.9 to -3.5 3.5 to 3.8
DJI S900 1	DJI S900	3.3 to 5.7
Indian Eagle Owl	Bird, Indian Eagle Owl	2.0 to 10
Test Datafile	**Target(s)**	**Velocity range (m/s)**
DJI S900 2 (Unseen)	DJI S900	2.0 to 3.6
Harris Hawk (Unseen)	Bird, Harris Hawk	-7.6 to -2.2

kept from one iteration to the next. This aims to limit oscillations in the training process due to the SGD algorithm. The network 'hyperparameters', such as the learning rate, size of hidden units, or dropout probability can also be changed. Trials to identify the optimal combination of these values were attempted, by checking the validation and test accuracies.

IV. LSTM TRAINING DATASET

The main goal whilst creating the labeled dataset for the supervised learning was to ensuring data diversity. Along with drone and bird data, noise and clutter data were also included to train the network for real scenario. Fig. 3 shows the variations in the drone and bird targets. A very low phase noise 94 GHz FMCW radar [17] was used for experimental data collection. The radar is circularly polarized (odd bounce). The set radar bandwidth during the trial was 150 MHz. The chirp period was 80.489 µs, corresponding to a CRF of 12.42

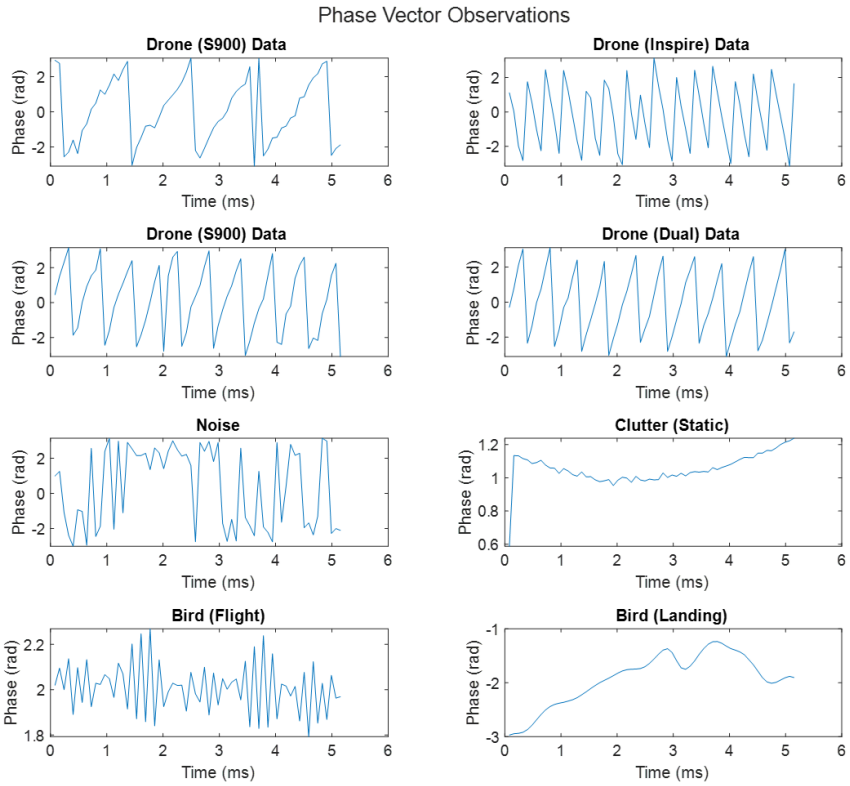

Fig. 6. Set of example phase vector sequences, labelled with their origin from the data available

kHz. Fig. 4 illustrates the phase sequence generation process. For the LSTM dataset, phase values of 64 contiguous chirps for a given range bin were selected, which corresponds to 5.15 ms. Fig. 5 shows an example RTI plot of two drones slowly flying in different directions at around 70 and 100 m range. Clutter returns at around 130-150 m range can also be seen. During the data labeling, these RTI plots were examined to select the range bins of interest. Range-Doppler plots were also generated for logging the detailed velocity information. It should be noted that these plots are used only to obtain the ground truth for the labeled data. As seen in Table II, the dataset includes phase values of varying bulk velocities, including drone hovering. The bird data also has variation in terms of wing flapping while landing or gliding. The final dataset created contained a total of 4800 phase vectors of length 64 chirps each. 2400 of these were 'drone' class, with 600 sequences from each of the four drone datafiles. 1200 sequences were taken from the Eagle Owl data as discussed above, and the remaining 1200 were taken from noise or clutter features throughout all five datafiles. This would provide a balance of the different features that were contained within the five sets of radar data. From Fig. 6, The different shapes for the drone and non-drone targets are clearly observable.

V. LSTM CLASSIFICATION RESULTS

Training and validation were done using the MATLAB training progress tool. This allowed a set of validation sequences and labels to be used to constantly check their classification accuracy, in addition to monitoring the training accuracy over time. Out of the 4800 sequences, 20% of each type were randomly selected to be set aside for this validation purpose. This number was chosen to keep enough samples available for training but having a range and quantity to check during the training process. 3840 sequences and their labels were split into mini-batches and used to train each network.

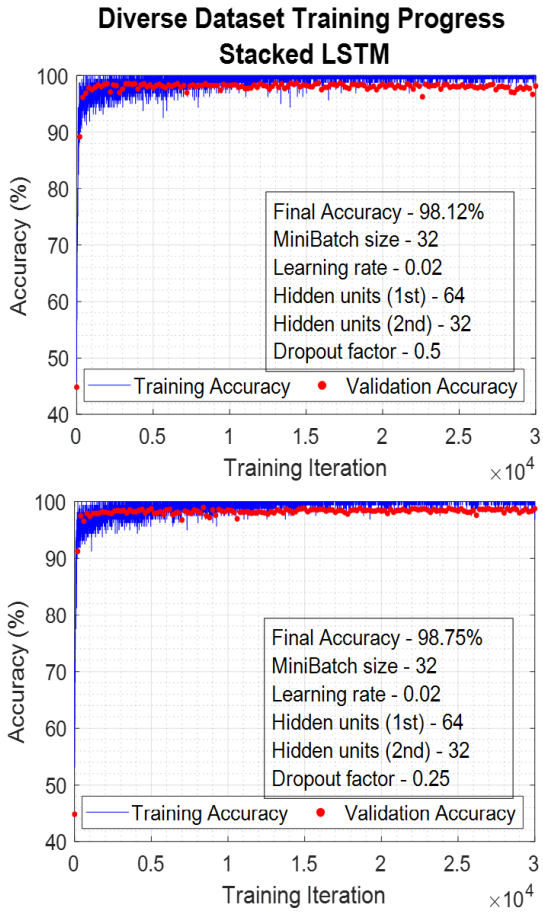

Fig. 7. Training and validation data for the stacked LSTM network with optimal parameters but different dropout factors

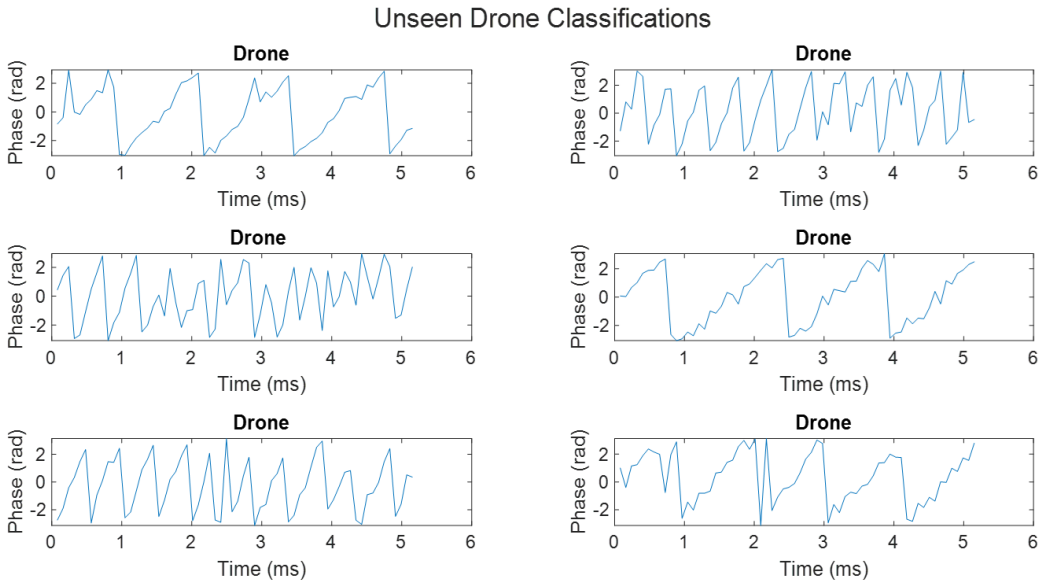

Fig. 8. Plot of the 6 randomly chosen drone sequences from the unseen data featuring DJI S900, all being correctly classified

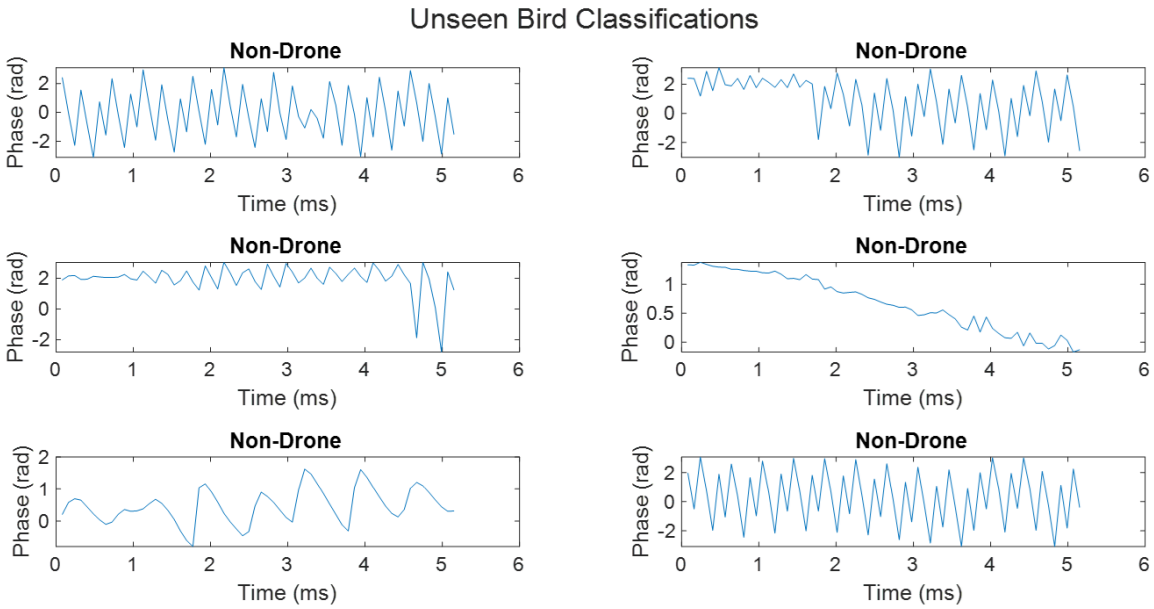

Fig. 9. Plot of the 6 randomly chosen bird sequences from the unseen data featuring Harris Hawk, all being correctly classified

The training was done using a GPU environment (GTX 970 or RTX 3070) in order to reduce the training time. The performance during training and validation for each version of the networks was recorded in addition to some variable values such as the mini-batch size and learning rate.

In addition to the validation performance, a key factor for each network was the performance when classifying completely unseen data. For this, the two unseen files shown in table II were used to create a labelled set of drone and non-drone phase vectors. In total, 600 drone, and a mix of 600 bird, noise and clutter sequences were labelled. A random subset of these were then given to the network to examine how successfully each vector was individually classified. The phase vectors were plotted with the classification from the network, and the confidence interval for the two types was recorded.

The stacked-LSTM network was then trained with the optimal parameters for learning rate and mini-batch size, whilst varying the dropout layer factor. Fig. 7 shows the parameter values, along with demonstrating that validation accuracies above 98% were achieved. Even though dropout factor of 0.25 gives better accuracy, the model with 0.5 dropout factor also performed very well with unseen data. Hence, it was selected as the final model as it should be less prone to overfitting.

An unseen dataset of 30 phase sequences was created, containing 10 randomly chosen sequences of drone, bird and noise/clutter labels. The network was able to classify both classes correctly in each case. The confidence level was no less than 0.89 in each case and more than 0.95 in most cases. Fig. 8 and Fig. 9 show examples of the performance of the LSTM network on unseen test data, showing correct classification in every case.

As all the phase vectors are generated from range transformed data, this allows for a significant reduction in time before classification by avoiding Doppler processing.

Performing the range transform on 64 chirps required 1.3 ms, compared to a range-Doppler transform which required 4.1 ms, and a full spectrogram generation which required 12 ms. This is a large advantage over existing spectrogram based classifiers when used in the context of a real-time drone detection, tracking and identification system.

VI. Conclusion

An LSTM based neural network is introduced with the goal to minimize the data processing time in a real-time drone classification by radar scenario. Basic simulation of phase sequences of micro-Doppler returns from a drone and a bird at 94 GHz was done, showing discernible features. A large and diverse dataset was then created for training, labeled with two classes, drone and non-drone. The validation and test accuracies on unseen data values are very promising, showing more than 98% accuracy in both cases. The time required for the classifier input data processing with this method is around factor of 10 faster than a spectrogram image based classification. This shows the potential for this technique to be explored on a real-time system, as it can be a very reasonable trade-off between the computational speed and a better classification performance from a more robust classifier.

As many commercial drone detection radars operate at lower frequencies, further investigation should be done to determine the efficacy of the network on radar data at those frequencies (e.g. X-band). Also, more drone data of different models including fixed wing types should help to improve the LSTM network to be more generalized.

Acknowledgment

The authors thank the contribution of the Elite Falconry for the bird data collection.

References

[1] I. Güvenç, O. Ozdemir, Y. Yapici, H. Mehrpouyan, and D. Matolak, "Detection, localization, and tracking of unauthorized UAS and Jammers," in *AIAA/IEEE Digital Avionics Systems Conference - Proceedings*, 2017, vol. 2017-Septe.

[2] J. S. Patel, F. Fioranelli, and D. Anderson, "Review of radar classification and RCS characterisation techniques for small UAVs or drones," *IET Radar, Sonar Navig.*, vol. 12, no. 9, pp. 911–919, Sep. 2018.

[3] G. Lykou, D. Moustakas, and D. Gritzalis, "Defending Airports from UAS: A Survey on Cyber-Attacks and Counter-Drone Sensing Technologies," *Sensors 2020, Vol. 20, Page 3537*, vol. 20, no. 12, p. 3537, Jun. 2020.

[4] W. Khawaja, M. Ezuma, V. Semkin, F. Erden, O. Ozdemir, and I. Guvenc, "A Survey on Detection, Tracking, and Classification of Aerial Threats using Radars and Communications Systems," *arXiv:2211.10038v1*, Nov. 2022.

[5] P. Molchanov, R. I. A. Harmanny, J. J. M. de Wit, K. Egiazarian, and J. Astola, "Classification of small UAVs and birds by micro-Doppler signatures," *Int. J. Microw. Wirel. Technol.*, vol. 6, no. 3–4, pp. 435–444, 2014.

[6] J. J. M. De Wit, R. I. A. Harmanny, and P. Molchanov, "Radar micro-Doppler feature extraction using the Singular Value Decomposition," in *2014 International Radar Conference, Radar 2014*, 2014.

[7] M. Ritchie, F. Fioranelli, H. Borrion, and H. Griffiths, "Multistatic micro-Doppler radar feature extraction for classification of unloaded/loaded micro-drones," *IET Radar, Sonar Navig.*, vol. 11, no. 1, pp. 116–124, Jan. 2017.

[8] P. Zhang, L. Yang, G. Chen, and G. Li, "Classification of drones based on micro-doppler signatures with dual-band radar sensors," in *Progress in Electromagnetics Research Symposium*, 2017, vol. 2017-November, pp. 638–643.

[9] S. Rahman and D. A. Robertson, "Classification of drones and birds using convolutional neural networks applied to radar micro-Doppler spectrogram images," *IET Radar, Sonar Navig.*, vol. 14, no. 5, pp. 653–661, May 2020.

[10] D. Raval, E. Hunter, S. Hudson, A. Damini, and B. Balaji, "Convolutional Neural Networks for Classification of Drones Using Radars," *Drones 2021, Vol. 5, Page 149*, vol. 5, no. 4, p. 149, Dec. 2021.

[11] H. Dale, M. Jahangir, C. J. Baker, M. Antoniou, S. Harman, and B. I. Ahmad, "Convolutional Neural Networks for Robust Classification of Drones," in *Proceedings of the IEEE Radar Conference*, 2022.

[12] D. A. Brooks, O. Schwander, F. Barbaresco, J. Y. Schneider, and M. Cord, "Temporal deep learning for drone micro-doppler classification," in *Proceedings International Radar Symposium*, 2018, vol. 2018-June.

[13] V. C. Chen, F. Li, S.-S. Ho, and H. Wechsler, "Analysis of micro-Doppler signatures," *IEE Proc. - Radar, Sonar Navig.*, vol. 150, no. 4, p. 271, 2003.

[14] V. C. Chen, *The micro-doppler effect in radar*. Artech House, 2011.

[15] S. Rahman and D. A. Robertson, "Millimeter-wave micro-Doppler measurements of small UAVs," in *Proc. SPIE 10188, Radar Sensor Technology XXI*, 2017, vol. 10188, p. 101880T.

[16] Staudemeyer, R.C., & Morris, E.R. (2019). Understanding LSTM - a tutorial into Long Short-Term Memory Recurrent Neural Networks. ArXiv, abs/1909.09586 .

[17] D. A. Robertson, G. M. Brooker, and P. D. L. Beasley, "Very low-phase noise, coherent 94GHz radar for micro-Doppler and vibrometry studies," in *Proc. SPIE 9077, Radar Sensor Technology XVIII*, 2014, vol. 9077, p. 907719.